

## Particle Stabilized Wet Foam to Prepare SiO<sub>2</sub>-SiC Porous Ceramics by Colloidal Processing

Subhasree Bhaskar, Jung Gyu Park, In Sub Han\*, Mi Jai Lee\*\*,  
Tae Young Lim\*\*, and Ik Jin Kim†

*Institute of Processing and Application of Inorganic Materials (PAIM), Department of Materials Science and Engineering,  
Hanseon University, Seosan 31962, Korea*

*\*Energy Materials Laboratory, Korea Institute of Energy Research (KIER), Daejeon 34129, Korea*

*\*\*Ceramics for Display & Optics, Korea Institute of Ceramic Engineering and Technology (KICET), Jinju 52851, Korea*

(Received September 4, 2015; Revised October 14, 2015; Accepted October 15, 2015)

### ABSTRACT

Porous ceramics with tailored pore size and shape are promising materials for the realization of a number of functional and structural properties. A novel method has been reported for the investigation of the role of SiC in the formation of SiO<sub>2</sub> foams by colloidal wet processing. Within a suitable pH range of 9.9 ~ 10.5 SiO<sub>2</sub> particles were partially hydrophobized using hexylamine as an amphiphile. Different mole ratios of the SiC solution were added to the surface modified SiO<sub>2</sub> suspension. The contact angle was found to be around 73°, with an adsorption free energy  $6.8 \times 10^{-12}$  J. The Laplace pressure of about 1.25 ~ 1.6 mPa was found to correspond to a wet foam stability of about 80 ~ 85%. The mechanical and thermal properties were analyzed for the sintered ceramics, with the highest compressive load observed at the mole ratio of 1:1.75. Hertzian indentations are used to evaluate the damage behavior under constrained loading conditions of SiO<sub>2</sub>-SiC porous ceramics.

**Key words :** Porous ceramics, Wet process, Adsorption free energy, Laplace pressure, Wet foam stability, Hertzian indentations

### 1. Introduction

Porous materials with controlled porosity usually exhibit specific properties such as low density, high permeability, high surface area, and good thermal insulation; these properties cannot be achieved by these materials' denser counterparts.<sup>1)</sup> Due to its excellent physical and chemical properties, SiO<sub>2</sub> powder has come to be increasingly attractive in and widely applied in many fields such as ceramics, catalyst carriers, chemical industries, solid fillers, and so on.<sup>2)</sup> Recently, for their high strength and excellent mechanical and chemical stability, SiC ceramics have been a focus of research in the field of porous ceramics.<sup>3)</sup> With the development of related science and technology, SiC can be considered a material with superior performance in high temperature applications<sup>4)</sup> including heat, corrosion, high thermal shock and wear resistance activities, along with strong antioxidant activity.<sup>5-7)</sup> This material can also be used in power devices, hot-gas or molten-metal filters, gas burner media, catalyst supports, thermal insulators, diesel engine exhaust gases, refractory materials, metal oxide semiconductor field effect transistors, etc.<sup>8-10)</sup>

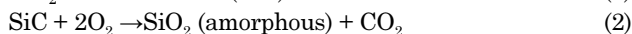
Solid state reaction techniques have been used in the preparation of SiC porous ceramics including the hot-pressing technique,<sup>11)</sup> dissolution-precipitation mechanisms,<sup>12)</sup> and the conventional sintering procedure.<sup>13)</sup> Controlling the morphological properties of materials during synthesis is of great importance, as these structural characteristics strongly influence material performance.<sup>14)</sup> Porous SiO<sub>2</sub>-SiC based ceramics can be fabricated by a variety of conventional methods such as replica, sacrificial template, direct foaming, freeze drying, sol-gel, bonding, and partial sintering techniques, among others.<sup>15-17)</sup>

Due to its inherent features such as versatility, simplicity, and low cost, the colloidal processing technique is suitable for preparing open and closed porous structures with the varied porosities used in our experiments. In this technique, air is directly incorporated into a suspension or liquid media by mechanical frothing, injection of a gas stream, gas-releasing chemical reactions, or solvent evaporation; the mixture is subsequently set in order to maintain the structure of the air bubbles that have been created.<sup>18)</sup> Long or short chain surfactants are used to reduce the free energy of the wet foams by lowering the air-water interface tension, increasing the surface viscosity and creating electrostatic forces to prevent the foam from collapsing.<sup>19-20)</sup>

In general, wet foams are thermodynamically unstable because of their large air-water interfacial area and resulting high adsorption free energy. To improve the stability of

†Corresponding author : Ik Jin Kim  
E-mail : [ijkim@hanseo.ac.kr](mailto:ijkim@hanseo.ac.kr)  
Tel : +82-41-660-1441 Fax : +82-41-688-1402

wet foams, particles have been used to adsorb at the air-water interface. The adsorption of particles reduces the highly energetic interfacial area and lowers the free energy of the system.<sup>21</sup> Due to the oxidative properties of SiC, Ar gas atmosphere has been used for sintering of dried porous ceramics to overcome the several possible oxidation reactions, such as:<sup>13, 21</sup>



The mechanical behavior of porous ceramics is greatly influenced by the material pore structure. The introduced porosity affects and alters the mechanical properties, making them different from those of dense ceramics. Therefore, mechanical measurement techniques commonly applied for dense ceramics might not be equally suitable for porous ceramics. Hertzian indentation is employed to investigate contact damage of porous SiO<sub>2</sub>-SiC ceramics.<sup>22-24</sup>

The objective of this work is to prepare SiC based porous ceramics by colloidal processing using surface modified SiO<sub>2</sub> as the basic functional material and SiC as an additive. The addition of SiC solution to the SiO<sub>2</sub> suspension resulted in a change in the wet-foam stability of the colloidal suspension. SiO<sub>2</sub> particles stabilize wet foams by causing steric hindrance to the coalescence of bubbles, and by modification of the colloidal properties of the interfaces.

## 2. Experimental Procedure

### 2.1. Raw materials

The experiments were carried out using high-purity SiO<sub>2</sub> (Cristobalite polymorph,  $d_{50} \sim 3.5 \mu\text{m}$ , > 99.0% purity, density  $\sim 2.65 \text{ g/cm}^3$ , Junsei Chemicals, Japan), SiC (Moissanite 6H polymorph, FCP 15C,  $d_{50} \sim 0.5 \mu\text{m}$ , > 99.0% purity, density  $\sim 3.21 \text{ g/cm}^3$ , SIKA Tech, Germany). Other chemicals used in the experiments were de-ionized water, hydrochloric acid (35% Yakuri Pure Chemicals, Osaka, Japan), sodium hydroxide powder (Yakuri Pure Chemicals, Kyoto, Japan) and Hexylamine (Alfa Aesar, Seoul, Korea).

### 2.2. Preparation of colloidal suspensions

The suspension was prepared by adding 50 vol.% of SiO<sub>2</sub> powder to SiC solution using 0.05 (M) Hexylamine as an amphiphile. Homogenization and de-agglomeration were performed using zirconia balls (10 mm diameter with 2:1 ratio of balls to powder). The pH values of the suspensions were initially fixed in a range of 9.9 ~ 10.5 while continuing the ball milling procedure for 24 ~ 48 h. The solid concentration of the SiO<sub>2</sub> suspension was reduced to 30 vol.% in order to maintain the stability of the airflow by decreasing the viscosity. The hexylamine concentration was adjusted to the required concentration in the final SiO<sub>2</sub> suspension for the partial hydrophobization of the particles. Meanwhile, the aqueous SiC solution was prepared at 10 vol.% solid loading by stirring to prevent oxidation of SiC during the ball mill-

ing process. Products of different mole ratios of SiO<sub>2</sub> suspension and SiC solutions were stirred uniformly for 10 ~ 15 min. to prepare the final suspension under constant atmospheric conditions.

### 2.3. Contact angle, surface tension and adsorption free energy

The pendant-drop-method (KSV Instruments Ltd, Helsinki, Finland) was used to measure the surface tension of the SiO<sub>2</sub>-SiC suspension, whereas the sessile-drop-method was used to measure the contact angle of the same. In the pendant-drop test, a drop of liquid is suspended from the end of a tube by surface tension. The force between the solid particles in the liquid phase, due to the surface tension, is proportional to the length of the boundary between the liquid and the tube, with the proportionality constant usually denoted by  $\gamma$ . Depending on the suspension contact angle and the surface tension, the drop volume generally varies between 5 and 10  $\mu\text{l}$ .

The variation in the stability of wet foam at the particle-stabilized interfaces is due to the adsorption free energy ( $\Delta G$ ) required to remove an adsorbed particle of radius  $r$  from an interface of surface tension  $\gamma\alpha\beta$ . This variation can be calculated using Eq. (1), where  $\theta$  is the contact angle ( $^\circ$ ) formed between the particle and the interface.<sup>25,26</sup>

$$\Delta G = \pi r^2 \gamma_{\alpha\beta} (1 - \cos\theta)^2 \quad \text{for } \theta \leq 90^\circ \quad (3)$$

According to the above equation,  $\Delta G(\text{J})$  is greatest when  $\theta$  is  $90^\circ$ ; however, foam stabilization of particles readily occurs when  $\theta$  is between  $50^\circ$  and  $90^\circ$ . Moreover, the stability of the thin liquid film between the air bubbles plays an important role in stabilizing wet foams, which decrease in thickness and eventually rupture due to foam drainage or to collisions between bubbles.

### 2.4. Foaming, air content and Laplace pressure

The foaming of 100 ml of each suspension was accomplished using a household hand mixer (150 W, Super Mix, France) at full power for 15 to 20 min. As shown in Fig. 1. the bubble size distribution of the foam was evaluated using an optical microscope in transmission mode (Somtech Vision, South Korea) with a connected digital camera, and measured using the software Linear Intercept (TU Darmstadt, Germany). The average bubble size was determined by the analysis of 100 bubbles in a composition.

The volume of air or voids in suspension in aggregate particles is called the air content (%) of the suspension, and is usually expressed as an increased percentage of the total volume of air in the mixture before and after foaming. The air content of an initial colloidal suspension measures the instance of the wet foam stability of a suspension. It can be measured by the following equation:

$$\text{Air Content (\%)} = \frac{(V_{\text{wet foam}} - V_{\text{suspension}})}{V_{\text{wet foam}}} \times 100 \quad (4)$$

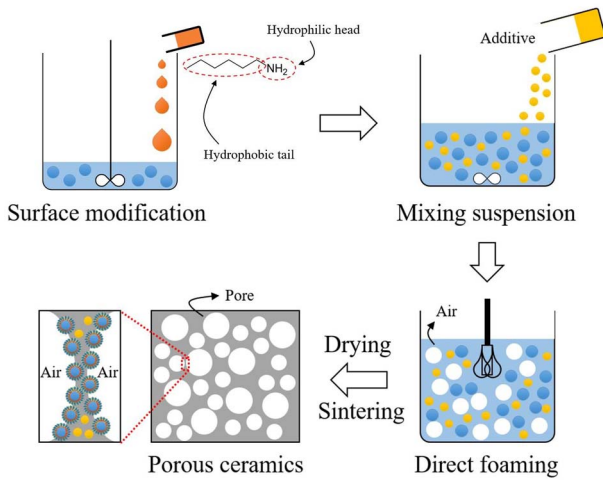


**Fig. 1.** Schematic representation of the preparation of SiO<sub>2</sub>-SiC porous ceramics from partially hydrophobized colloidal suspension.

Where,  $V_{wet\ foam}$  is the volume of the ceramic wet foam after foaming and  $V_{suspension}$  indicates the volume of the suspension before foaming.<sup>27)</sup>

Furthermore, due to the steady diffusion over time of gas molecules from smaller to larger bubbles, a broadening of the bubble size distribution occurs. The difference in the Laplace pressure between bubbles of distinct sizes ( $R$ ) leads to bubble disproportionation and Ostwald ripening. Due to the combined actions of these destabilization mechanisms, the liquid foam collapses. The pressure acting on the gas bubbles in a colloidal suspension can be described by the Laplace pressure as:

$$\Delta P = \gamma \left( \frac{1}{R_1} + \frac{1}{R_2} \right) = \frac{2\gamma}{R} \quad (\text{For spherical bubble}) \quad (5)$$

Where,  $\Delta P$  = Laplace pressure (mPa) is the pressure difference between the inner and outer surfaces of a bubble or droplet, this effect is caused by the surface tension  $\gamma$  (mN/m) at the interface between the liquid and the gas.  $R_1$  and  $R_2$ , the radii of curvature for an ellipse, are taken into consideration. However, for spherical bubbles,  $R_1$  and  $R_2$  are equal, so we used the second formula for calculation of the Laplace pressure.<sup>28)</sup>

### 2.5. Drying and sintering

Wet samples were dried at 50°C for 24 ~ 48 h. in a sterilizer. The dried foams were sintered in a super kantal furnace (max. 1650°C) at 1500°C for 1 h. in an argon atmosphere with rates of heating and cooling of 1°C/min and 3°C/min, respectively, due to the oxidation problem of SiC into SiO<sub>2</sub>, as mentioned earlier in the reactions shown in Eqs. (1) & (2).

### 2.6. Wet foam stability

The total porosity of sintered ceramics is proportional to

the quantity of bubbles incorporated into the suspension during the foaming process. Wet foam stability (%) can be defined by the reduction of the volume of a foams after it is dried at room temperature (20 ~ 25°C), and can be represented by Eq. (7).

$$\text{Wet foam stability (\%)} = \left( \frac{V_{final}}{V_{initial}} \right) \times 100 \quad (6)$$

Where,  $V_{final}$  indicates the volume of the ceramic foam after drying and  $V_{initial}$  is the volume of the ceramic wet foam.<sup>28)</sup>

### 2.7. Mechanical testing

The mechanical behavior of the load-displacements curve of the sintered SiO<sub>2</sub>-SiC porous ceramics was investigated using Hertzian indentations tests. Cylindrical specimens of 2.54 cm, diameter x 1 cm thickness were cut from the as-received materials and polished. Hertzian indentation tests were performed in air with a universal testing machine (Model 5567, Instron Corp., Canton, MA) at a constant cross-head speed of 0.2 mm/min over a load range of  $P = 5\text{--}200$  N, using tungsten carbide spheres of radius  $r = 7.93$  mm. The compressive load vs. displacement curves were plotted during loadings and unloadings. The displacements were converted through an amplifier, converters, and a digital signal processor, consecutively, after measurement by the extensometer.

## 3. Results and Discussion

Controlling the contact angle of particles at interface is one of the most important aspects of applying processing routes in the synthesis of porous materials. The contact angle of colloidal particles at a fluid interface depends on the surface chemistry, roughness, impurities, and particle size, as well as on the composition of the fluid phases.<sup>29)</sup> The degree of particle hydrophobization achieved through the surface adsorption of amphiphiles was investigated with the help of surface tension measurements. A decrease in the surface tension upon increasing the initial additive concentration is observed for the evaluated suspensions.<sup>18)</sup>

Contact angles of particles at an interface determine the wetting ability according to the extent that the particles are hydrophobic, as shown in Fig. 2. The average contact angle of the colloidal suspension was found to increase from 55° ~ 73° with the increase in the mole ratio of SiC to 1:1.25. However, a lower range of contact angle has been observed with further increases in the SiC content. This is due to the increase in the viscosity of the particles in the colloidal suspension. Moreover, the surface tension of the suspension (the contractive tendency of the outer surface of the liquid) decreases at the same mole ratio of about 1 : 1.25 to around 60 mN/m, at which point the wet foams were found to be the most stable. Further, with the increase in the SiC content, the foams were observed to gradually increase, which leads to lower wet foam stability.

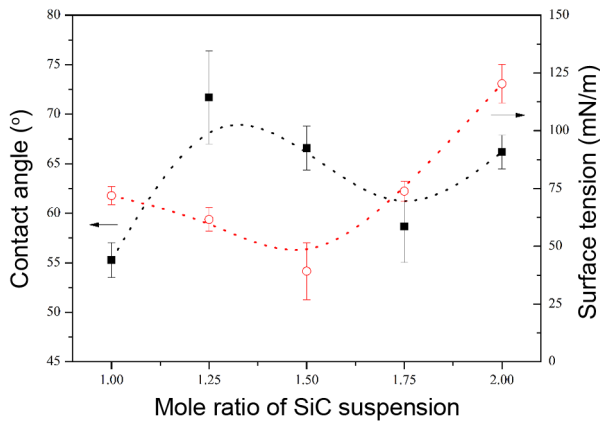


**Fig. 2.** Contact angle and surface tension of colloidal suspension with respect to mole ratio of SiC.

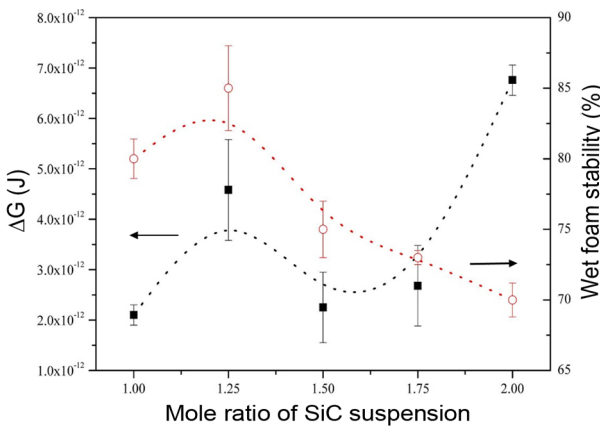


**Fig. 3.** Adsorption free energy vs. wet foam stability with respect to the mole ratio of SiC in the colloidal suspension.

The adsorption free energy of surfactant adsorption is the surface excess of the Gibbs thermodynamic potential and is widely used as a basic thermodynamic characteristic of surfactants.<sup>30)</sup> Fig. 3 shows the change in adsorption free energy in relation to the wet foam stability with respect to the SiC content when hexylamine (0.05 M) was used to partially hydrophobize the initial SiO<sub>2</sub> suspensions. This can be interpreted as showing that there is an increase in the free energy ( $2.0 \times 10^{-12} \sim 4.2 \times 10^{-12}$  J), as well as an increase in the wet foam stability to around 85% with the increase in the mole ratio to 1:1.25, as per Eq. (4), with the increase in the contact angle (when the radius of the SiO<sub>2</sub> particle was calculated, the contact angle and surface tension were measured using the sessile-drop method and the pendant-drop method, respectively). With the further increase in the SiC content, the free energy were found to decrease gradually. Henceforth, it can be proved that the ratio of 1 : 1.25 is the most stable zone for the wet foams in our experiment.

The air content, calculated as per Eq. (4), of an initial colloidal suspension indicates the wet foam stability of a suspension. In Fig. 4, the air content of the suspension initially decreases from 60 ~ 33% with the increase in the SiC con-

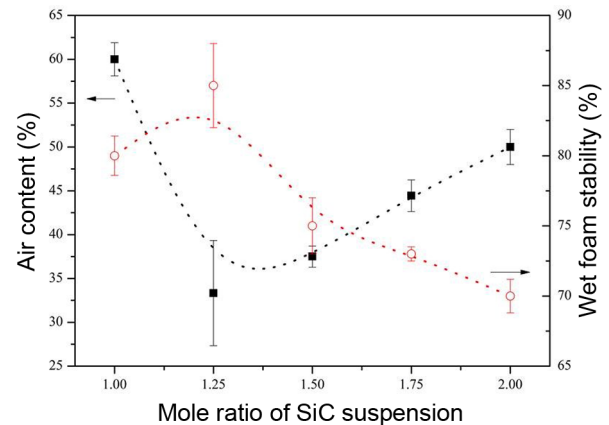


**Fig. 4.** Air content vs. wet foam stability with respect to the mole ratio of SiC.

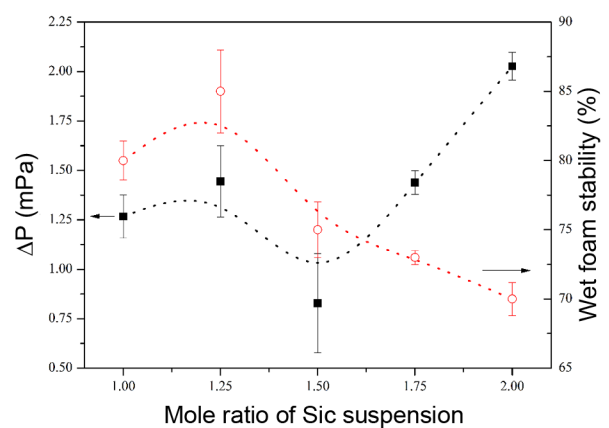


**Fig. 5.** Laplace pressure vs. wet foam stability with respect to the mole ratio of SiC.

tent to 1:1.25. The wet foam stability has been found to be the highest at this mole ratio. Moreover, with the increase in the SiC content, the air content was found to increase simultaneously as the wet foam stability decreases. This is due to the increase in the excess air incorporation into the suspension; the bubbles tend to collapse, which leads to irreversible destabilization mechanisms like Ostwald ripening, drainage, and coalescence of the bubbles.<sup>21)</sup> Hence, it can be interpreted that the air content of the colloidal suspension is inversely proportional to the wet foam stability of the porous ceramic foam.

Figure 5 shows the wet foam stability, which corresponds to the Laplace pressure exerted by the bubbles of the wet-foams formed with respect to the particle concentration. This stability value can be calculated using Eq. (5) (in which the surface tension is measured by the pendant-drop method and the radii of the larger and smaller bubbles are measured by optical microscopy). The difference in pressure initially increased as the bubble size decreased (as shown in Fig. 6); the stability also increased to around 85% in a pressure range of about 1.25 ~ 1.6 mPa, which corresponds to an SiC content of 1:1.25 mole ratio. Further increases in the

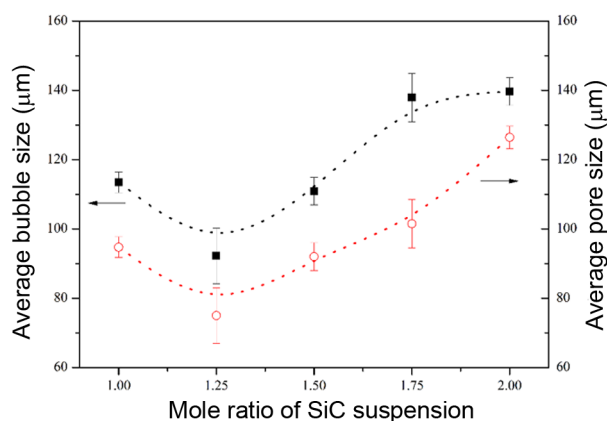


Fig. 6. Average bubble size vs. average pore size with respect to the mole ratio of SiC.

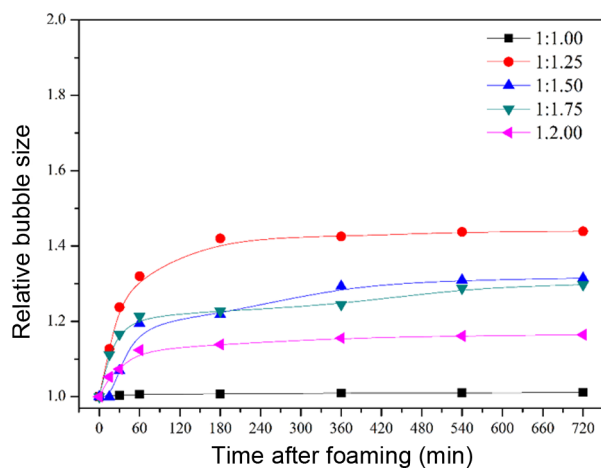


Fig. 7. Relative average bubble size of SiO<sub>2</sub>-SiC ceramic wet foams with respect to the time after colloidal processing.

solid loading resulted in a lowering of the Laplace pressure as well as resulting in a corresponding wet-foam stability, because these properties are inversely related to the average bubble size of the wet foams.

In Fig. 6, the bubble size increased gradually from 92 ~ 113 μm with increasing of the mole ratio of SiC in the colloidal suspension from 1:1 to 1:1.25. The bubble size increases gradually with further increase in the mole ratio of SiO<sub>2</sub>-SiC. Similarly, the pore size decreased gradually to 78 μm with increasing SiC content, which gradually increases with further increase in content of the same in the colloidal suspension. This proves the effect of the Laplace pressure (as shown in Fig. 5), which is inversely related to the average bubble size. The bubble size and pore sizes of the wet and dry foams were found to be 92 μm and 78 μm, respectively, at the mole ratio of SiO<sub>2</sub> to SiC of 1:1.25, with the highest wet foam stability showing a value of around 85%.

Figure 7 shows the relative bubble size with respect to time when, after 1 h, the bubbles tend to collapse due to Ostwald ripening, with a gradual increase in the bubble

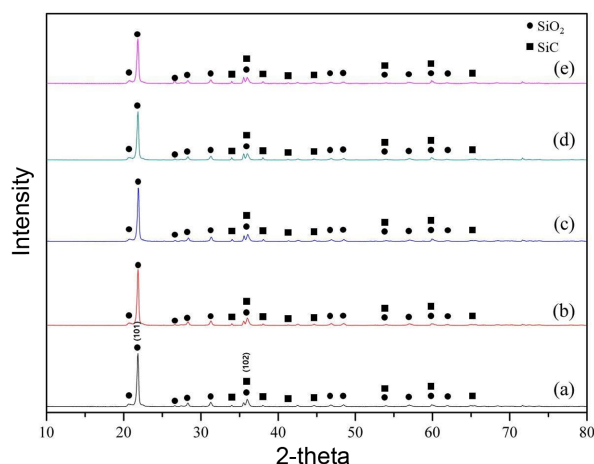


Fig. 8. XRD patterns for SiO<sub>2</sub>-SiC porous ceramics: (a) 1 : 1, (b) 1 : 1.25, (c) 1 : 1.50, (d) 1 : 1.75, and (e) 1 : 2, sintered at 1500°C in Ar atmosphere for 1 h.

size. At the mole ratio of SiO<sub>2</sub>-SiC of 1:1.25, there is a maximum relative increase in the bubble size, with the highest wet foam stability, as has been shown in the previous results. On the other hand, the mole ratios of 1 : 1.5 and 1 : 1.75 were found to lead to drastic increases in the relative bubble size with respect to time because of the excess of SiC particles in the ceramic suspension. Hence, from the above figure we can infer that the SiC content is an important parameter for the stability of wet foams.

In Fig. 8, showing results of the XRD analysis of the crystalline phase, the patterns point to a high crystallinity for all SiO<sub>2</sub>-SiC porous ceramics. The observed Bragg peaks can undoubtedly be identified as SiC for the samples of different mole ratios of the SiO<sub>2</sub>-SiC suspension. Fig. 8 shows the XRD patterns of the SiO<sub>2</sub>-SiC porous ceramics sintered at 1500°C in argon atmosphere with different mole ratios; in these cases, the SiO<sub>2</sub> used was in cristobalite form and the SiC used was in the Moissanite 6H form of a polymorph. From the XRD patterns for all the mole ratios of SiC, the peaks for both SiO<sub>2</sub> and SiC can be seen. The observed Bragg peaks can undoubtedly be identified for the samples of different mole ratios of the SiO<sub>2</sub>-SiC suspension. The main intensity peaks of the different composites were identified, with a peak at 22 degrees (hkl = 101) for the cristobalite phase and one at 35.2 degrees (hkl = 102) for the SiC phase. This proves that, in the presence of Ar atmosphere, the oxidation of SiC into SiO<sub>2</sub> can be prevented. As we gradually increase the percentage of SiC in the samples with higher mole ratios, the material retains SiC in the sintered porous ceramics.

In Fig. 9 plots for the compression load vs. the displacement curve can be observed with respect to the different mole ratios of SiO<sub>2</sub>-SiC. The compression load seems to increase with the increase in the displacement as well as with the increase in the mole ratio. The highest compressive load was observed to be around 45 N, with a displacement of around 1.6 mm, at the mole ratio of 1 : 1.75. In spite of hav-



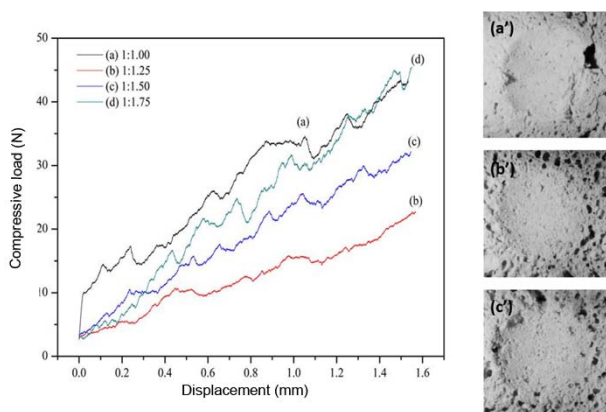


**Fig. 9.** Compression load vs. displacement curve for the different mole ratios of SiC; 9(a'), 9(b'), and 9(c') provide optical images of the damaged surfaces of the SiO<sub>2</sub>-SiC porous ceramics of mole ratios of 1 : 1, 1 : 1.5, and 1 : 1.75, respectively.

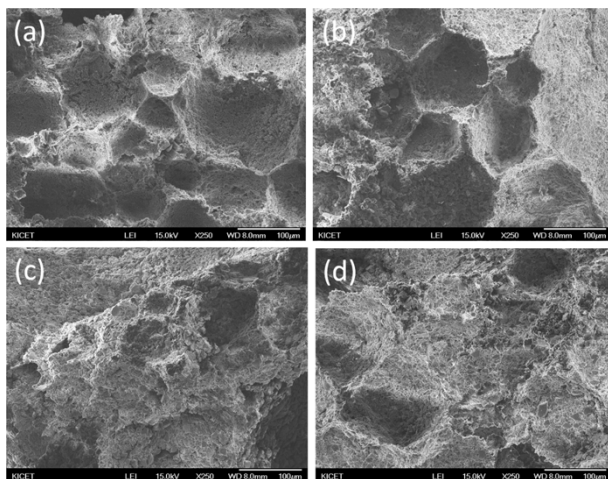


**Fig. 10.** Microstructure of porous ceramics of 30 vol.% SiO<sub>2</sub> with respect to the different mole ratios of SiC: (a) 1 : 1.25, (b) 1 : 1.50, (c) 1 : 1.75, and (d) 1 : 2, sintered at 1500°C in Ar atmosphere.

ing the highest wet foam stability, the 1 : 1.25 mole ratio was found to have mechanical properties that were relatively low. Figs. 9(a'), 9(b'), and 9(c') provide optical images of the damaged surfaces of the different mole ratios of the SiO<sub>2</sub>-SiC porous ceramics. Fig. 9(a') shows the damaged surface clearly, with definite cracks on the surface. However, the damaged surface becomes more prominent in Figs. 9(b) and 9(c').

In Fig. 10, the microstructure exhibits variable patterns of pore size distribution of the larger and smaller closed pores. The porous ceramics in Fig. 10(a) and 10(b) are shown in enlarged view, in which can be seen their larger sized pores. The rough and uneven distribution of pores along the surface of the sintered ceramics can also be seen. The magnified views in Fig. 10(c) and 10(d) show a hierarchical pore-distribution from larger to smaller pores. The corresponding increase in the pore size of the sintered ceramics with the

bubble size of the wet foam (if we compare with Fig. 6) can be interpreted as showing a lower chance of incidence of destabilization mechanisms.

## 4. Conclusions

The stability of a ceramic foam is directly related to the surface energy of a colloidal suspension. This helps in the calculation of the free energy and the Laplace pressure for the corresponding interface-contact angle. We conclude that a stabilizing point can be obtained for the production of porous ceramics. This stabilization point can be tailored by adjusting the solid content of the suspension, which is directly related to the free energy and the Laplace pressure and which is in the range of 1.25 ~ 1.6 mPa; this range corresponds to the wet-foam stability range of sintered porous ceramics. Wet-foam stability of around 85% was established, corresponding to a particle free energy of  $4.2 \times 10^{-12}$  J. The highest compression load was observed at around 45 N, with a displacement of around 1.6 mm at the mole ratio of 1:1.75.

## Acknowledgments

The authors would like to thank Hanseo University, Korea, the Korea Institute of Ceramic Engineering and Technology (KICET), and the Korea Institute of Energy Research (KIER) for supporting this research both technically and financially.

## REFERENCES

1. X. Wang, J. Liu, F. Hou, X. Lu, X. Sun, and Y. Zhou, "Manufacture of Porous SiC/C Ceramics with Excellent Damage Tolerance by Impregnation of LCPS into Carbonized Pine-wood," *J. Eur. Ceram. Soc.*, **35** 1751-59 (2015).
2. X. Shen, Y. Zhai, Y. Sun, and H. Gu, "Preparation of Monodisperse Spherical SiO<sub>2</sub> by Microwave Hydrothermal Method and Kinetics of Dehydrated Hydroxyl," *J. Mater. Sci. Tech.*, **26** [8] 711-14 (2010).
3. S. Liu, Y. P. Zeng, and D. Jiang, "Fabrication and Characterization of Cordierite-Bonded Porous SiC Ceramics," *Ceram. Intl.*, **35** 597-602 (2009).
4. S. P. Lee, J. O. Jin, and A. Kohyama, "Fabrication and Properties of Reaction Sintered SiC Based Materials," *Key Eng. Mater.*, **261-63** 1475-80 (2004).
5. B. Liu, "Properties and Manufacturing Method of Silicon Carbide Ceramic New Materials," *Appl. Mech. Mater.*, **416-17** 1693-97 (2013).
6. S. Suyama and Y. Itoh, "Strengthening Mechanism of High-Strength Reaction-Sintered Silicon Carbide," *Key Eng. Mater.*, **484** 89-97 (2011).
7. Y. Hirata Y, N. Matsunaga, and S. Sameshima, "Densification, Phases, Microstructures and Mechanical Properties of Liquid Phase-Sintered SiC," *Key Eng. Mater.*, **484** 124-29 (2011).
8. Q. Liu, F. Ye, Y. Gao, S. Liu, H. Yang, and Z. Zhou, "Devel-

- opment of Elongated 6H-SiC Grains in Reaction-Bonded Porous SiC Ceramics," *Scr. Mater.*, **71** 13-16 (2014).
9. T. Ujihara, R. Maekawa, R. Tanaka, K. Sasaki, K. Kuroda, and Y. Takeda, "Stability Growth Condition for 3C-SiC Crystals by Solution Technique," *Mater. Sci. Forum.*, **600-03** 63-6 (2009).
  10. J. Li, H. Lin, and J. Li, "Factors that Influence the Flexural Strength of SiC-based Porous Ceramics Used for Hot Gas Filter Support," *J. Eur. Ceram. Soc.*, **31** 825-31 (2011).
  11. Y. Hirata, N. Matsunaga, N. Hidaka, T. Maeda, T. Arima, S. Sameshima, "Improvement of Strength, Weibull Modulus and Damage Tolerance of SiC," *Mater. Sci. Forum.*, **561-65** 489-94 (2007).
  12. Y. Hirata, N. Matsunaga, N. Hidaka, S. Tabata, and S. Sameshima, "Processing of High Performance Silicon Carbide," *Key Eng. Mater.*, **403** 165-68 (2009).
  13. K. Biswas, "Solid State Sintering of SiC-Ceramics," *Mater. Sci. Forum.*, **624** 71-89 (2009).
  14. B. Wu, R. Yuan, and X. Fu, "Structural Characterization and Photocatalytic Activity of Hollow Binary ZrO<sub>2</sub>/TiO<sub>2</sub> Oxide Fibers," *J. Solid State Chem.*, **182** 560-65 (2009).
  15. X. Wang, K. Wang, J. Kong, Y. Wang, and L. An, "Synthesis of Non-Oxide Porous Ceramics Using Random Copolymers as Precursors," *J. Mater. Sci. Tech.*, **31** [1] 120-24 (2015).
  16. Y. W. Kim, C. Wang, and C. B. Park, "Processing of Porous Silicon Oxycarbide Ceramics from Extruded Blends of Polysiloxane and Polymer Microbead," *J. Ceram. Soc. Jpn.*, **115** [7] 419-24 (2007).
  17. J. H. Eom, Y. W. Kim, and S. Raju, "Processing and Properties of Macroporous Silicon Carbide Ceramics: A Review," *J. Asian Ceram. Soc.*, **1** 220-42 (2013).
  18. A. R. Studart, U. T. Gonzenbach, E. Tervoort, and L. J. Gauckler, "Processing Routes to Macroporous Ceramics: A review," *J. Am. Ceram. Soc.*, **89** [6] 1771-89 (2006).
  19. U. T. Gonzenbach, A. R. Studart, E. Tervoort, and L. J. Gauckler, "Stabilization of Foams with Inorganic Colloidal Particles," *Langmuir*, **22** 10983-88 (2006).
  20. A. Pokhrel, D. N. Seo, T. L. Seung, and I. J. Kim, "Processing of Porous Ceramics by Direct Foaming: A Review," *J. Korean Ceram. Soc.*, **50** [2] 1-10 (2013).
  21. S. Bhaskar, G. Y. Cho, J. G. Park, S. W. Kim, H. T. Kim, and I. J. Kim, "Micro Porous SiO<sub>2</sub>-SiC Ceramics from Particle Stabilized Foams by Direct Foaming," *J. Ceram. Soc. Japan*, **123** [5] 378-82 (2015).
  22. B. R. Lawn, N. P. Padture, H. Cai, and F. Guiberteau, "Making Ceramics 'Ductile'," *Science*, **263** 1114-6 (1994).
  23. H. Cai, M. A. S. Kalceff, and B. R. Lawn, "Deformation and Fracture of Mica Containing Glass-Ceramics in Hertzian Contacts," *J. Mater. Res.*, **9** 762-70 (1994).
  24. B. R. Lawn, "Indentation of Ceramics with Spheres: a Century after Hertz," *J. Am. Ceram. Soc.*, **81** 1977-94 (1998).
  25. S. Bhaskar, J. G. Park, S. W. Kim, H. T. Kim, and I. J. Kim, "Effect of Surfactant on Adsorption Free Energy and Laplace Pressure on Wet Foam Stability to Porous Ceramics," *J. Ceram. Pro. Res.*, **16** [1] 1-4 (2015).
  26. S. Bhaskar, J. G. Park, G. Y. Cho, S. Y. Kim, and I. J. Kim, "Wet Foam Stability and Tailoring Microstructure of Porous Ceramics using Polymer Beads," *Adv. Appl. Ceram.*, **114** [6] 333-37 (2015).
  27. W. Zhao, S. Bhaskar, J. G. Park, S. Y. Kim, I. S. Han, and I. J. Kim, "Particle-Stabilized Wet Foams to Porous Ceramics by Direct Foaming," *J. Ceram. Pro. Res.*, **15** [6] 503-7 (2014).
  28. S. Bhaskar, J. G. Park, G. Y. Cho, D. N. Seo, and I. J. Kim, "Influence of SiO<sub>2</sub> Content on Wet Foam Stability for Creation of Porous Ceramics," *J. Korean Ceram. Soc.*, **51** [5] 511-14 (2014).
  29. A. R. Studart, U. T. Gonzenbach, I. Akartuna, E. Tervoort, and L. J. Gauckler, "Materials from Foams and Emulsions Stabilized by Colloidal Particles," *J. Mater. Chem.*, **17** 3283-89 (2007).
  30. K. D. Danov and P. A. Kralchevsky, "The Standard Free Energy of Surfactant Adsorption at Air/Water and Oil/Water Interfaces: Theoretical vs. Empirical Approaches," *Colloid Journal*, **74** [2] 172-85 (2012).